Available online at www.sciencedirect.com
SCIENCE DIRECT
Cement and Concrete Research 36 (2006) 521 – 529
Cement and Concrete Research

Evaluation on steel bar corrosion embedded in antiwashout underwater concrete containing mineral admixtures

Han Young Moon, Kook Jae Shin *

Hanyang University, Department of Civil Engineering, 17 Haengdang-Dong, Seongdong-Gu, Seoul 133-791, Republic of Korea

Received 28 November 2004; accepted 14 September 2005

Abstract

This study aims the evaluation of the corrosion of steel bar embedded in antiwashout underwater concrete, which has rather been neglected to date. To that goal, accelerated steel bar corrosion tests have been performed for three series of steel bar-reinforced antiwashout underwater concrete specimens manufactured with different admixtures and under different environments. The three series of antiwashout underwater concrete were: concrete constituted exclusively by ordinary portland cement (OPC), concrete composed by ordinary portland cement mixed with fly-ash in 20% ratio (FA20) and concrete with ground granulated blast furnace slag is mixed in 50% ratio (BFS50). And, the three different environments were: manufacture in the air, in tap water, and in artificial seawater.

Measurement results using half-cell potential surveyor showed that, among all the specimens, steel bar in OPC manufactured in artificial seawater was the first one that exceeded the threshold value proposed by ASTM C 876 with a potential value below −350 mV after 14 cycles. And, the corresponding corrosion current density and concentration of water soluble chloride were measured as 0.3 $\mu A/cm^2$ and 0.258%. On the other hand, for the other specimens that are FA20 and BFS50, potential values below −350 mV were observed later at 18 and 20 cycles, respectively.

Results confirmed the expectation that mineral admixtures may be more effective in delaying the development of steel bar corrosion in antiwashout underwater concrete.

Keywords: Antiwashout underwater concrete; Half-cell potential value; Corrosion current density; Water soluble chloride

1. Introduction

Antiwashout underwater concrete is by nature used essentially in aquatic environment and is increasingly finding most of its applications in marine environment rather than fresh water or river. In Korea, antiwashout underwater concrete has been applied on the foundations of Seohae Bridge, Youngjong Bridge and Gwangan Bridge, which is actually under construction in Suyeong Bay in the city of Busan. However, differently from antiwashout underwater concrete structures constructed in fresh water or in river, the structures built under marine environment are showing significant loss of durability and one main reason of such loss of performance is the penetration of Cl^- ion included in seawater. Particularly, Cl^- ions infiltrated inside concrete cause embedded steel bar to corrode and instigate cracks to develop, of which extent affects sensitively the durability of concrete.

Up-to-date, numerous researches have been led to evaluate properties of antiwashout underwater concrete like its segregation degree, fluidity and compressive strength, but their scope remain limited to basic properties without or with very little regard to its durability. In view of such circumstances, researches on the corrosion of reinforcing bar are thus inexistent.

Since its invention, about 35 years ago in Germany, antiwashout underwater concrete has seen continuous evolution. Sogo et al. in 1987 attempted to increase its resistance against washout by adding polymer [1]. Thereafter, in 1990, Hara et al. succeeded in improving its fundamental properties by mixing of ground granulated blast furnace slag [2]. Hara found out that the titrated rate of substitution ranged between 40% and 50%. Especially, Khayat et al. published his first treatise on antiwashout underwater concrete in 1995 followed

* Corresponding author. Tel.: +82 2 10 9108 7778; +82 2 2205 1123.
E-mail address: rickyshin@hotmail.com (K.J. Shin).

0008-8846/$ - see front matter © 2005 Elsevier Ltd. All rights reserved.
doi:10.1016/j.cemconres.2005.09.014

Table 1
Chemical compositions and physical properties of cement and mineral admixtures (%)

	SiO_2	Al_2O_3	Fe_2O_3	CaO	MgO	SO_3	Ig. loss	Specific gravity	Specific surface area (cm^2/g)
OPC	21.95	6.59	2.81	60.10	3.32	2.11	2.58	3.15	3112
FA	67.70	25.00	2.85	2.00	0.90	–	3.47	2.15	3274
BFS	32.30	14.80	0.40	44.10	5.50	1.00	1.10	2.80	4580

by many other ones and, contributed effectively to the development of fluidity and self-compacting properties of antiwashout underwater concrete [3–7]. Unfortunately, most of these papers focused essentially on the fundamental properties of antiwashout underwater concrete such as fluidity, filling-up performance and application of mineral additives, neglecting the durability aspect.

With these regards, this study takes place in the framework of endurance evaluation of antiwashout underwater concrete. In this study, corrosion tests of steel bar embedded in antiwashout underwater concrete were performed and data were examined. The natural electric potential and the corrosion current density of steel bar were measured during 24 cycles using a half-cell potential surveyor and guard ring device. The amount of soluble chloride and the rate of corroded area were finally calculated and processed. In addition, several preliminary tests were carried out to verify the fundamental properties of antiwashout underwater concrete.

2. Experimental procedures

2.1. Materials

Ordinary portland cement (OPC, type 1) usually manufactured in Korea was used as basic cementitious material, and fly-ash (FA) and ground granulated blast furnace slag (BFS) were employed as supplementary cementitious materials. The chemical compositions and physical properties of cement and mineral admixtures are shown in Table 1.

Well-graded crushed stone aggregates and siliceous sand with a fineness modulus of 2.83 were used. Their physical properties are summarized in Table 2.

The liquid-based cellulosic anti-washout underwater admixture (AWA) and the melamine-based high range water reducer (HRWR) presented specific gravities of 0.8 and 1.23 respectively, with the properties listed in Table 3.

For the reinforcement, smoothed steel bar with a diameter of 13 mm was employed and its chemical composition is given in Table 4. Before being embedded in concrete, the bar was brushed with No. 200 sandpaper and cleaned with acetone.

Table 2
Physical properties of aggregates

	Specific gravity	Absorption (%)	Percentage of solids (%)	F.M.	Abrasion value (%)	Unit weight (kg/m^3)
Fine aggregate	2.59	0.80	56.4	2.83	–	1473
Coarse aggregate	2.66	0.78	64.9	6.51	28.6	1741

Table 3
Physical properties of chemical admixtures

	Main composition	Specific gravity	Dosage (%)	Appearance
AWA	HPMC	0.8±0.1	1.0–1.2 (×W)	White powder
HRWR	Melamine	1.23±0.02	1.8–2.1 (×C)	Transparent liquid

2.2. Preparation of specimen

For the experiments, three series of antiwashout underwater concrete were mixed: (1) concrete constituted exclusively by ordinary Portland cement (OPC), (2) concrete composed by ordinary Portland cement mixed with fly-ash in 20% ratio (FA20) and (3) concrete in which ground granulated blast furnace slag is mixed in 50% ratio (BFS50). Three different processes were also used to prepare the concretes: manufacture (1) in the air, (2) in tap water, and (3) in artificial seawater. The general cast method of antiwashout underwater concrete is depicted in Fig. 1. For the steel bar corrosion test specimen, smoothed steel bar with a diameter of 13mm has been embedded in each specimen, excluding the preliminary test specimen for which no steel bar has been employed. The details of the specimen are shown in Fig. 2. To measuring the amount of water soluble chloride, manufactured specimen was coated with epoxy on the whole surface excluding the one crossed section, so the unidirectional penetration of chloride was allowed. The measurements of the amount of water soluble chloride were performed after 14 and 24 cycles of test. The mixture proportions adopted for each series are arranged in Table 5. All specimens for both preliminary and corrosion tests were taken out form those mold after 48 h, followed by standard curing until the next test.

2.3. Test techniques

2.3.1. pH and suspended solids

Underwater dropping test were performed in accordance with the guidelines proposed by the Korean society of civil engineers (KSCE). The test begins by filling a 1000 ml beaker with 800 ml of distilled water. Then, 500 g of antiwashout underwater concrete being dropped into the filled beaker, 600 ml of the upper water is extracted using a pipette. The quantities of suspended solids are measured by suction using 400 ml of the extracted water passed through filter paper. The remaining 200 ml are finally used to measure the pH by means of pH meter.

Table 4
Chemical compositions of rebar (%)

C	Si	Mn	P	S	Ni	Cr	Mo	Cu	Sn
0.24	0.23	0.95	0.016	0.008	0.03	0.04	0.01	0.02	0.0005

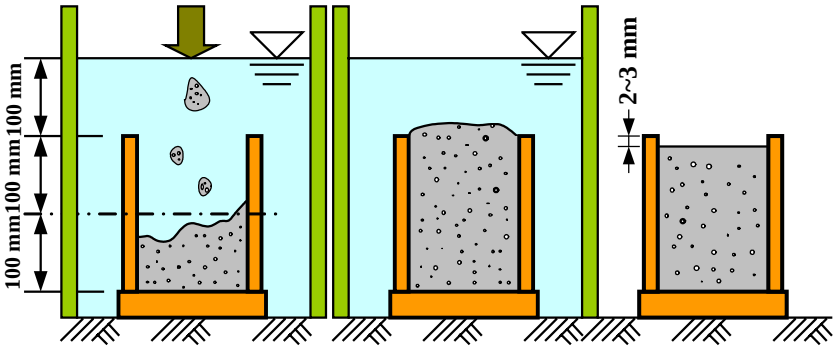

Fig. 1. The manufacture method of antiwashout underwater concrete (for the manufacture of air based specimen, water was removed and for the seawater based specimen the tap water was replaced by artificial seawater).

2.3.2. Slump flow and L-flow test

In order to evaluate the fluidity of antiwashout underwater concrete, slump-flow and L-flow test has been conducted immediately after the mixing. The L-flow test process is illustrated graphically in Fig. 3. As shown in Fig. 3, L-flow box test involves filling concrete on one side of the box and then opening a gate to allow the concrete to flow in water. It measures the fluidity of concrete in water by measurement of the time required to flow by a definite distance that is 400 mm in this case.

2.3.3. Accelerated corrosion test of steel bar

For the accelerated corrosion test, 2× concentration of artificial seawater based on ASTM D 1141 was employed. After 14 days of standard curing, the specimens were immersed during 3 days in 2× concentration of artificial seawater and dried for 4 days at ambient temperature. The test was conducted for 24 cycles and 1 cycle was readjusted with 3 days wetting and 4 days drying.

2.3.4. Half-cell potential test

In conformity with ASTM C876, the corrosion potential (E_{corr}) was measured by means of half-cell potential surveyor. The reference electrode (RE) was provided by a saturated copper sulfate electrode (CSE). Measuring procedure was performed after every 2 cycles of test (before immersion for the next cycle) and Fig. 4 schematizes the test method using half-cell potential surveyor.

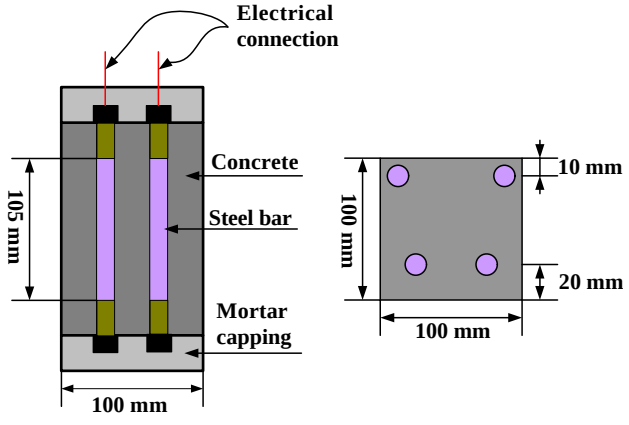

Fig. 2. Schema of steel bar corrosion specimen.

2.3.5. Corrosion current density (I_{corr})

A guard ring device was used to measure I_{corr} since the reliability of its performance has been recognized by Strategic Highway Research Program (SHRP) [8]. After every 2 cycles of test, all specimens were soaked by spraying distilled water and the measuring procedure for I_{corr} was conducted. For the calculation of I_{corr}, the Stern–Geary relation Eq. (1) [9] was employed.

$$I_{corr} = \frac{B}{R_p} \tag{1}$$

where $B=(\beta_a\beta_c)/[2.3(\beta_a+\beta_c)]$, and β_a and β_c are the anodic and cathodic Tafel constants, respectively.

The manual of the guard ring device suggests the value of B as 26 mV and, also for the reinforcing steel embedded in concrete, the value of B is recommended as 26 mV [10,11]. This technique has been reported to produce accurate results [12–14]. The value of the steel bar area used for the calculation of I_{corr} was 42.9cm^2. The process of the test method is illustrated in Fig. 5.

2.3.6. Amount of water soluble chloride

Prepared specimen is drilled at various locations to produce powdered samples that are collected. Then, according to the recommendations of the Japan Concrete Engineering Association related to the evaluation procedure of salt content in reinforced concrete, salt solution is extracted so as to measure the ratio of cement weight and chloride amount (Cl^- %) with the chloride ion detector using selective ion electrode.

Table 5
Mixture proportions of each series

	W/Cm (%)	S/a (%)	Air (%)	Unit weight (kg/m^3)						AWA (W × %)	HRWR (C × %)
				W	C	G	S	FA	BFS		
OPC	50	42	4±1	210	420	938	674	–	–	1.20	1.80
FA20	50	42	4±1	210	336	918	660	84	–	1.20	1.80
BFS50	50	42	4±1	210	210	924	664	–	210	1.20	1.80

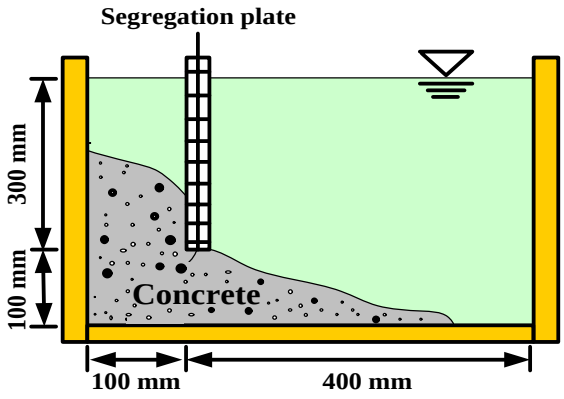

Fig. 3. Details of L-flow test.

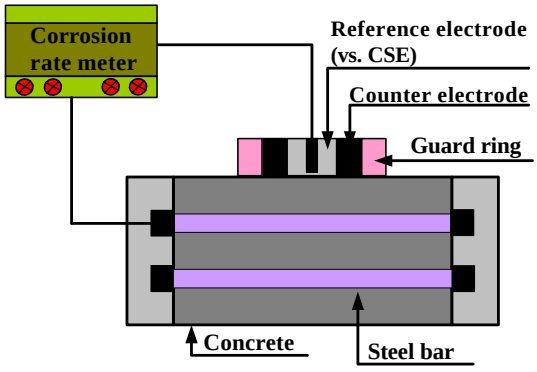

Fig. 5. Schematic details of guard ring device test.

3. Preliminary test results

Figs. 6, 7 and 8 depict the test data to evaluate the fundamental properties of antiwashout underwater concrete in various compositions of concrete before performing corrosion test of steel bar.

3.1. pH and suspended solids

Fig. 6 depicts the changes of pH and mass of suspended solids when antiwashout underwater concrete is mixed with mineral admixtures. Generally, underwater concrete losses its original quality during construction because cement is washed off and diluted by water flow. In addition, underwater concrete affects the ecological system around the construction site since it contaminates water. Therefore, the resistance of antiwashout underwater concrete against washout is evaluated through comparative tests on its pH and mass of suspended solids. As described in Fig. 6, the specimen in which fly-ash and ground granulated blast furnace slag is blended has a slightly lower pH. This result suggests that the mineral additive agent substitutes partially the cement portion, which means reduction of cement content and in turn decreases pH.

For the mass of suspended solids, OPC presents 65 mg/l while fly-ash and ground granulated blast furnace slag specimens exhibit 118 mg/l and 81 mg/l, respectively. Consequently, it can be assumed that the non-hydraulic property of fly-ash and ground granulated blast furnace slag causes the amount of suspended solids to increases. Especially, fly-ash is seen to have the largest mass of suspended solid. This can be explained by the adsorption of antiwashout underwater agent by non-combusted carbons, which releases significantly binder particles. However, the KSCE recommended pH and mass of suspended solids below 12 and 150 mg/l in its "Quality specifications for antiwashout underwater agent." Following, any caution about the applicability of antiwashout concrete could not be issued since test results satisfied these standards.

3.2. Slump flow and elapsed time

Compaction of antiwashout concrete is mostly impossible since it is mainly constructed under water. Therefore, differently from ashore concrete, higher fluidity and self-compacting property are necessarily required. In this study, a melamine-based high performance water reducer is used to improve the fluidity of antiwashout underwater concrete with cellulose based antiwashout underwater admixture. Fig. 7 illustrates the effect of mineral additive on fluidity of antiwashout underwater concrete. It is seen that antiwashout underwater concrete exhibit better slump flow and elapsed time (time to reach 400 mm) if the amount of mineral additive is increased. Consequently, it can be deduced that the globular shaped particles of fly-ash work as a ball bearing or that the glassy surface texture of ground granulated blast furnace slag helps fresh concrete to flow.

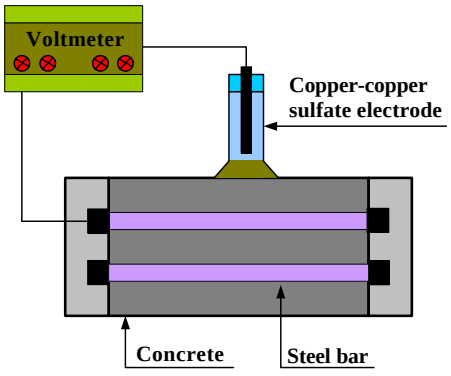

Fig. 4. Schematic details of the half-cell potential test.

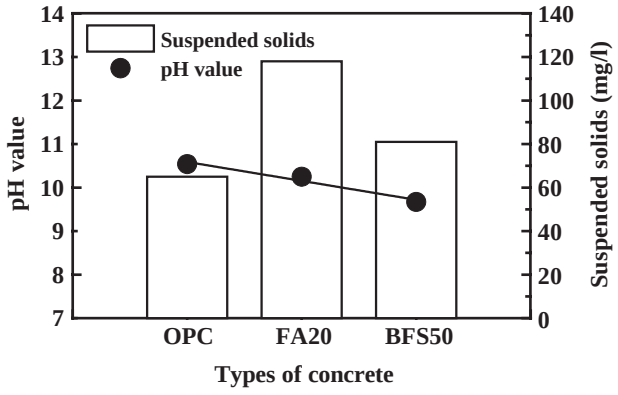

Fig. 6. The pH and suspended solids of antiwashout underwater concretes.

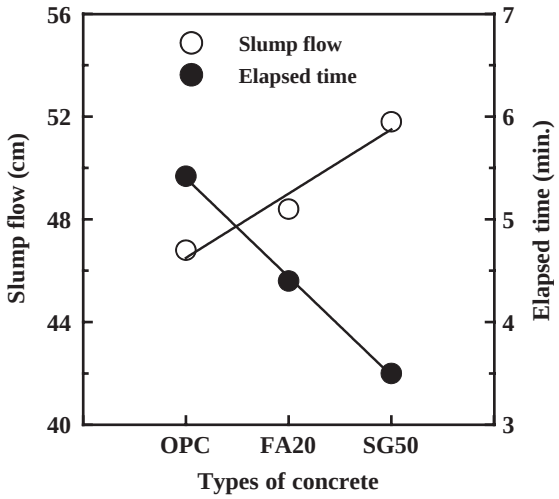

Fig. 7. Fluidity of antiwastout underwater concretes.

3.3. Compressive strength

Fig. 8 plots the evolution of the percentage of compressive strength of OPC to FA20 and BFS50 to represent the effect of mineral additive on the compressive strength of antiwashout underwater concrete. The dashed line represents the strength of OPC. It is seen that the 3 test cases exhibit similar evolution of compressive strength even if different procedures have been applied to manufacture the concrete specimens.

On the other hand, until 28 days of curing, OPC showed the largest compressive strength characteristic in every specimen. However, by passing 91 days of curing, this situation has been reversed. At 91 days, FA20 showed compressive strength higher by 2% to 10.8% compared to OPC and BFS50 presented strength larger by 5% to 13.8% compared to OPC. Finally, it can be concluded that even if the introduction fly-ash and ground granulated blast furnace slag mitigates the initial strength compared to OPC, this strength tends to increase to become higher than OPC in a long-term. This progress is well known as pozzolan reaction and potential hydrate property.

4. Steel bar corrosion test: results and discussion

4.1. Electrochemically measured E_{corr} and I_{corr}

Figs. 9, 10 and 11 illustrate the values of E_{corr} in each cycle for OPC, FA20 and BFS50. All the tested specimens showed distinctive threshold values of corrosion for 1 cm and 2 cm of concrete cover. If the corrosion threshold potential value of steel bar is −350 mV, CSE (with respect to copper/copper sulfate electrode) as proposed by ASTM C 876, the reinforcing bar with 2 cm of concrete cover exhibits the most stable potential value range (−200 mV ~−350 mV), compared to 1 cm of concrete cover. As a matter of fact, increasing the thickness of concrete cover is the best solution to slow down corrosion. However, this method is out-of-date being economically onerous.

On the other hand, as shown in Fig. 9, potential below −350 mV began to appear after 14 cycles (98 days) for OPC specimen with concrete cover of 1 cm and manufactured under artificial seawater. This specimen was the first one to exceed the corrosion threshold potential. This can be explained by the fact that the specimen has been manufactured under seawater, which mobilized a large quantity of chloride ions contained in seawater and therefore accelerated the appearance of corrosion. Similar trend has been observed in the test data of FA20 and BFS50 (Figs. 10 and 11).

Fig. 12 summarizes separately the half-cell potential value of steel bar-reinforced antiwashout underwater concrete prepared under artificial seawater. The potential reaches a value below −350 mV at 18 cycles (126 days) for FA20 and 20 cycles (140 days) for BFS50. That is it has only arrived to the value of threshold potential for high probability of corrosion activity, which is −350 mV, CSE with respect to copper/copper sulfate electrode [15,16]. The starting point of corrosion may thus be delayed in some extent by the mineral admixtures. Similar results were obtained for the corrosion current density summarized in Fig. 13, which is the results of specimens manufactured under artificial seawater. The slope of corrosion current density tends to become lower successively for OPC, FA20 and BFS50. At 14 cycles, corresponding to the time when potential becomes lower than −350 mV in steel bar with 1 cm of concrete cover, the corrosion current densities of OPC, FA20 and BFS50 approach 0.3, 0.26 and 0.2 μA/cm^2, respectively. According to the Strategic Highway Research Program (SHRP), it is reported that when corrosion current density ranges between 0.2 μA/cm^2 and 0.5 μA/cm^2, the corrosion has begun or is going to begin.

Several researchers have considered values of current density greater than 0.3 μA/cm^2 to be indicative of active corrosion [17,18]. Andrade and Alonso have provided a set of value for the levels of corrosion rate. They considered that

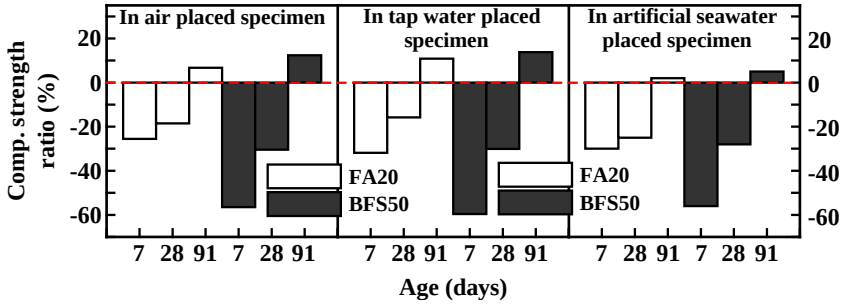

Fig. 8. The characteristic of compressive strength development of antiwashout underwater concrete containing mineral admixtures.

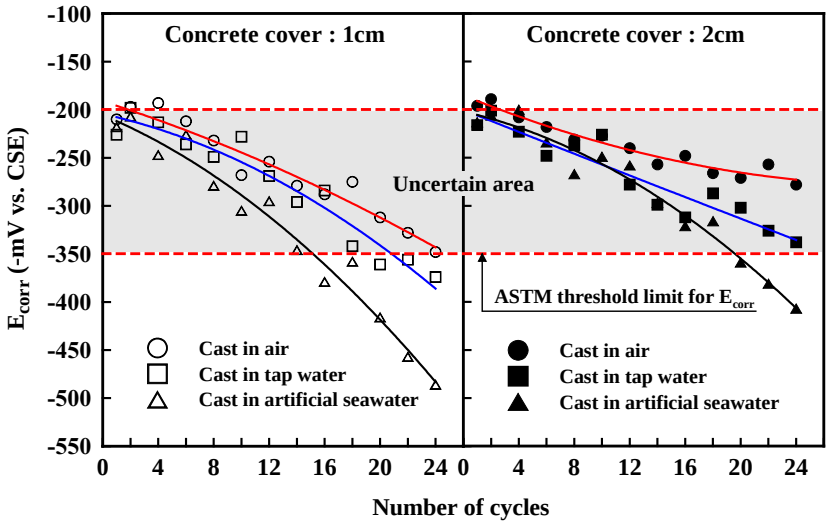

Fig. 9. E_{corr} vs. number of cycles for OPC.

corrosion current density of 0.1 to 0.5 μA/cm^2 is low and 0.5 to 1 μA/cm^2 is moderate. Values above 1 μA/cm^2 are considered high while below 0.1 μA/cm^2 are deemed negligible [11,19]. Gonzalez et al. [19] concluded that corrosion current density less than 0.1 to 0.2 μA/cm^2 would be acceptable with no durability risks.

Consequently, even if the more conservative value of 0.2 is adopted, OPC and FA20 already exceeded the corrosion threshold value and BFS50 just reached the corrosion threshold value. However the half-cell potential values of FA20 and BFS50 measured at 14 cycles were −305 mV and −302 mV, respectively, and did not exceed the corrosion threshold limit proposed by ASTM C 876 (Fig. 12). Hence, it is verified that the more moderate value of 0.3 μA/cm^2 is more acceptable to evaluate steel bar corrosion of antiwashout underwater concrete. In conformity with Al Amoudi et al. [18], it can be concluded the value 0.3 μA/cm^2 is more appropriate for the threshold value for active reinforcement corrosion. However, further and deeper researches will be needed for assessment of steel bar corrosion in antiwashout underwater concrete.

The relationship between corrosion current density and half-cell potential value during the cycles of exposure to accelerated corrosion test is shown in Fig. 14. It is seen here that a corrosion current density of 0.2 and 0.3 μA/cm^2 is associated with the half-cell potential threshold value of −350 mV, CSE. From the results in Fig. 14, a relationship between corrosion current density (I_{corr}) and half-cell potential (E_{corr}) for OPC with concrete cover of 1cm could be expressed by:

$$I_{corr} = 0.342 \times \ln(E_{corr}) - 1.712 \quad (2)$$

Within 24 cycles (168 days) of accelerated corrosion test, corrosion current density reaching almost 0.4 μA/cm^2 could be predicted from this relationship only for OPC-based antiwashout underwater concrete. On the other hand, Fig. 14 shows that corrosion current density and half-cell potential value for BFS50 remained at a relatively low level throughout the testing periods. It should be stressed that the special ingredients for

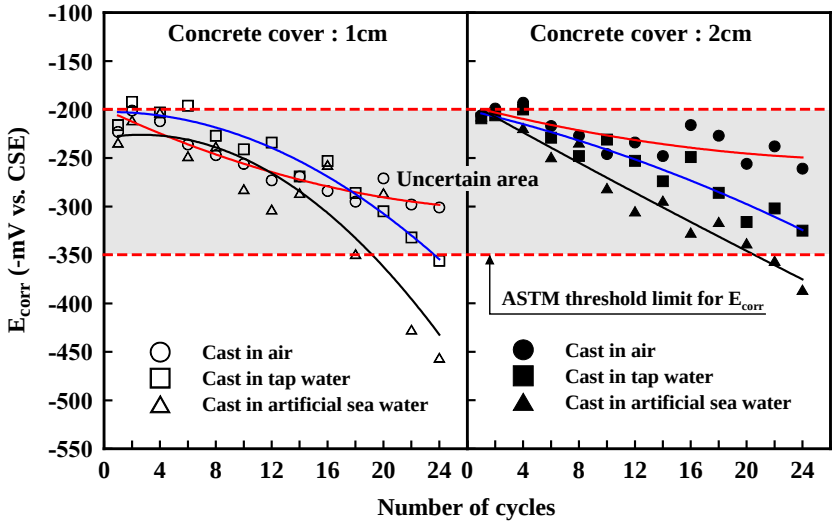

Fig. 10. E_{corr} vs. number of cycles for FA20.

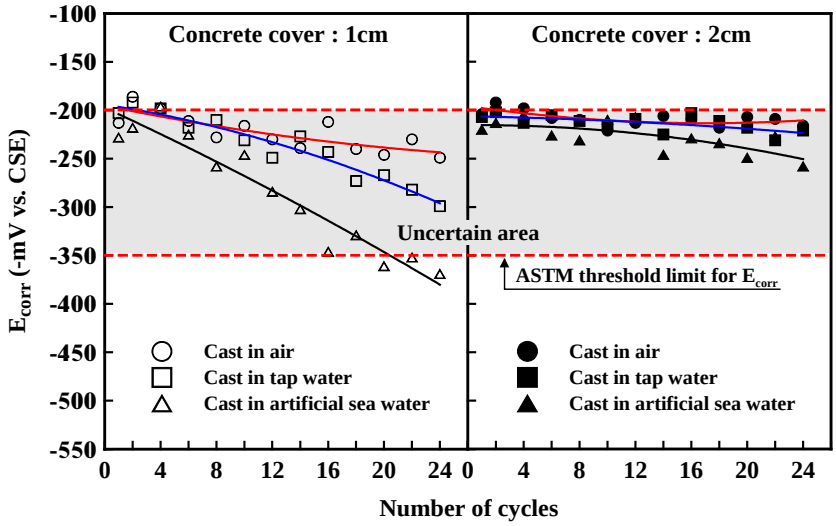

Fig. 11. E_{corr} vs. number of cycles for BFS50.

durable antiwashout underwater concrete such as ground granulated blast furnace slag may result in particular effects on performance.

4.2. Soluble chloride contents

The "water soluble" chloride ion penetration profile of antiwashout underwater concrete manufactured under artificial seawater is illustrated in Fig. 15. It is seen here that the water soluble chloride contents of OPC-based antiwashout underwater concrete measured at 14 cycles was around 0.258% (at 1 cm) while 0.146% and 0.129% in antiwashout underwater concrete prepared by mixing fly-ash and ground granulated blast furnace slag, respectively. This trend can be explained by the fact that fly-ash and ground granulated blast furnace slag induce pozzolan reaction and potential hydraulic property and so-generated compact C–S–H hydrates fill the capillary pore which is the main migration channel of chloride.

In the meantime, the value of 0.258% for OPC-based antiwashout underwater concrete is exceeding the critical limit of 0.15% proposed by ACI 318-89. In other words, this means that corrosion of steel bar has already proceeded to some extent in conformity with ACI 318-89. With this point, a comparison with the half-cell value of OPC could happen accidentally and a misled conclusion could be obtained that the critical limit of 0.15% proposed by ACI 318-89 may be slightly conservative for critical limit of antiwashout underwater concrete, because the value of half-cell potential for OPC with 1 cm of concrete cover barely reached −350 mV, CSE after 14 cycles.

However, it is necessary to keep in mind that the E_{corr} is qualitative measure, while the value of I_{corr} is a quantitative measure and therefore the latter is more important for the interpretation of the results.

Accordingly, the relationship between the corrosion current density and the amount of water soluble chloride is illustrated in Fig. 16 and from this figure misled hypothesis could be corrected. In Fig. 16, a clear linear relationship between the value of I_{corr} and the Cl^- (%) is detected, expressed by:

$$I_{corr} = 0.8008 \times Cl^-(\%) + 0.1097,\ r^2 = 0.8724 \quad (3)$$

This kinetics indicates that the steel is active, since an increase in the Cl^- (%) it supposes an increment in the I_{corr},

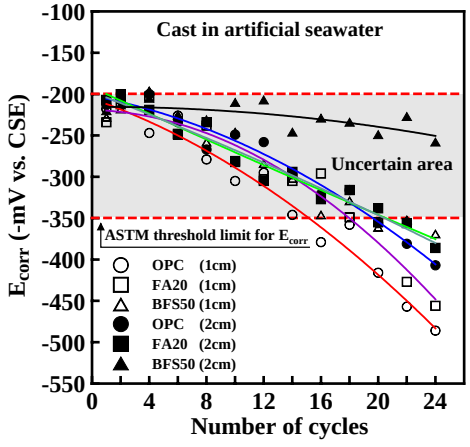

Fig. 12. E_{corr} vs. number of cycles for specimens cast in artificial seawater.

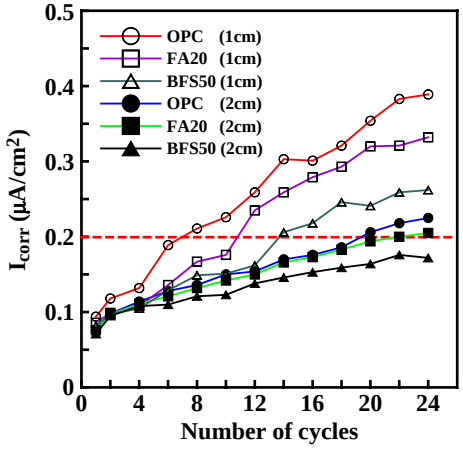

Fig. 13. I_{corr} vs. number of cycles for specimens cast in artificial seawater.

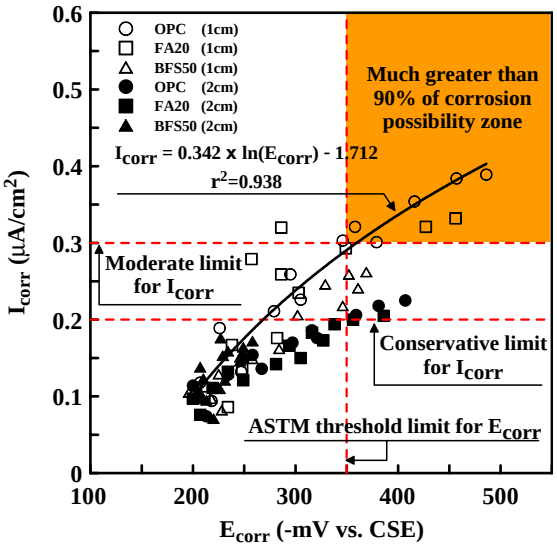

Fig. 14. I_{corr} vs. E_{corr} for specimens cast in artificial seawater.

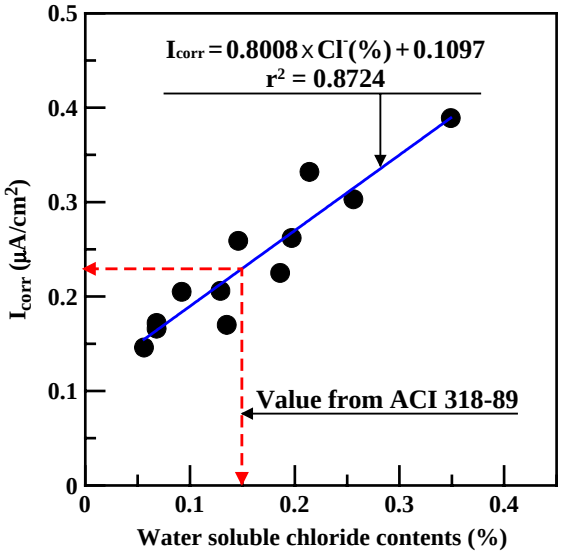

Fig. 16. Relationship between Cl^- (%) vs. I_{corr}.

although for the lowest values in the content in chlorides the corresponding values of corrosion do not represent durability risks. In this expression, it is indicated that for the value of 0.15% proposed by ACI 318-89 it corresponds to a value of 0.23 μA/cm^2, which justifies that indicated by Andrade et al. [11,17–19] when they concluded "that corrosion current density less than 0.1 to 0.2 mA/cm^2 would be acceptable with no durability risks".

5. Conclusions

1. From preliminary test results, it has seen that antiwashout underwater concrete specimens with fly-ash in 20% ratio (FA20) satisfied the criterion recommended by KSCE (150 mg/l) even if they presented the largest mass of suspended solid due to the action of non-combusted carbons. In addition, fluidity tests showed that antiwashout underwater concrete exhibit better slump flow and elapsed time if the amount of mineral additive is increased. Concerning the compressive strength, OPC showed the largest value until 28 days. But, after 91 days, it was observed that the action of fly-ash and ground granulated blast furnace slag continuously increased so that FA20 exhibited performance larger by 2% to 10.8% compared to OPC. In the case of BFS50, the highest increase was observed with an amelioration of compressive strength by 5% to 13.8%. Fly-ash and ground granulated blast furnace slag were thus seen to increase significantly compressive strength in a long-term.
2. From the accelerated corrosion test, it was observed that the specimens manufactured in seawater tend to develop corrosion of steel bar earlier. This can be explained by the mobilization of a large quantity of chloride ions contained in artificial seawater which accelerated the appearance of corrosion.
3. In the case of OPC manufactured in artificial seawater, the potential of steel bar with 1 cm thick concrete cover was the first one to exceed the threshold value with −350 mV after 14 cycles, while steel bar in FA20 and BFS50 reached −350 mV at 18 and 20 cycles, respectively. This verified that mineral admixtures retarded the development of corrosion in steel bar.
4. When potential below −350 mV were observed at 14 cycles, the corrosion current densities measured in steel bar embedded in OPC, FA20 and BFS50 were 0.3 μA/cm^2, 0.26 μA/cm^2 and 0.2 μA/cm^2, respectively. The corresponding potentials of FA20 and BFS50 were −305 mV and −302 mV, which did not reach the threshold value. Following, a threshold of 0.3 μA/cm^2 can be considered as an acceptable value when evaluating the corrosion state of steel bar-reinforced antiwashout underwater concrete by means of corrosion current density measured by guard ring device. Nevertheless, deeper researches are needed to correlate field and laboratory results.
5. The amount of soluble chloride measured at 14 cycles for OPC at a depth of 1 cm was 0.258% while 0.146% and

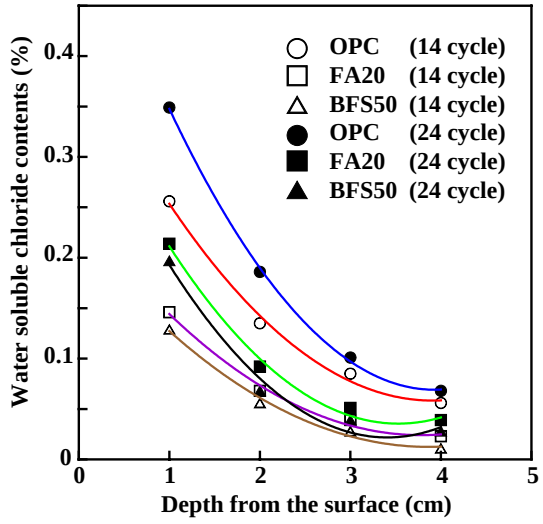

Fig. 15. Chloride concentration profile and regression curves for specimens cast in artificial seawater at 24 cycles of test.

0.129% in FA20 and BFS50, respectively. This trend can be explained by the pozzolan reaction and potential hydraulic property and so-generated compact C–S–H hydrates fill the capillary pore which is the main migration channel of chloride. In the meantime, from Eq. (3), it is clearly confirmed that the very close relationship between the value of I_{corr} and the amount of water soluble chloride exists.

6. After completion of the 24 cycles planned experimentation it is confirmed that the ground granulated blast furnace slag and fly-ash are effective in increasing the resistance of steel bar-reinforced antiwashout underwater concrete against corrosion.

References

[1] S. Sogo, T. Haga, T. Nakagawa, Fifth International Congress on Polymers in Concrete, Brighton, England, September, 1987.
[2] M. Hara et al., Admixing effect of high fineness slag on the properties of underwater concrete, Admixtures for Concrete, Improvement of Properties, E. Vazquez, editor, Chapman and Hall, London, 1990.
[3] K.H. Khayat, ACI Mater. J. 92 (2) (1995) 164.
[4] K.H. Khayat, ACI Mater. J. 93 (2) (1996) 134.
[5] M. Sonebi, K.H. Khayat, ACI Mater. J. 98 (M26) (2001) 233.
[6] K.H. Khayat, M. Sonebi, ACI Mater. J. 98 (M31) (2001) 289.
[7] K.H. Khayat, J. Assaad, ACI Mater. J. 100 (M21) (2003) 185.
[8] F. Janusz, S. Akshey, L. Dan, D. Philip, Method for Measuring the Corrosion Rate of Reinforcing Steel, SHRP-S/FR-92-104, Strategic Highway Research Program, vol. 2, National Research Council, Washing, DC, 1992.
[9] M. Stern, A.L. Geary, J. Electrochem. Soc. 104 (1) (1957) 56.
[10] C. Andrade, V. Castelo, C. Alonso, J.A. Gonzalez, ASTM Special Technical Publication STP 906, American Society for Testing and Materials, Philadelphia, 1986, p. 63.
[11] C. Andrade, C. Alonso, Constr. Build. Mater. 15 (2–3) (2001) 141.
[12] J.P. Broomfield, J. Rodriguez, L.M. Ortega, A.M. Garcia, Structural Faults and Repair, University of Edinburgh, 1993, p. 155.
[13] S. Feliu, C. Gonzalez, J. Feliu, M.C. Andrade, ACI Mater. J. 87 (5) (1990) 457.
[14] S. Feliu, C. Gonzalez, C. Andrade, V. Feliu, Corrosion 44 (10) (1988) 761.
[15] J.P. Broomfield, A. Anguilar, A.A. Sagues, R.G. Powers, in: N.S. Berke, V. Chaker, D. Whiting (Eds.), Corrosion Rates of Steel in Concrete, ASTM STP, vol. 1065, American Society for Testing and Materials, Philadelphia, 1990, p. 66.
[16] D. Baweja, H. Roper, V. Sirivivatnanon, The Australia–US workshop on High Performance Concrete, Curtin University, Perth, 1997, p. 411.
[17] C. Andrade, C. Alonso, J.A. González, in: N.S. Berke, V. Chaker, D. Whiting (Eds.), Corrosion Rates of Steel in Concrete, ASTM STP, vol. 1065, American Society for Testing and Materials, Philadelphia, 1990, p. 29.
[18] O.S.B. Al-Amoudi, M. Maslehuddin, A.N. Lashari, A.A. Almusallam, Cem. Concr. Comp. 25 (4–5) (2003) 439.
[19] J.A. Gonzalez, S. Feliu, P. Rodriguez, E. Ramirez, C. Alonso, C. Andrade, Mater. Struc. 29 (1996 (January–February)) 40.